Chapter 2
Nanostructures in Materials Subjected to Severe Plastic Deformation

As was already noted above, the first observations of the production of Ultrafine-grained materials (UFG) microstructures in bulk materials using the 'top-down' approach appeared in the scientific literature in the early 1990s in several publications by Valiev et al. dealing with pure metals and alloys [1, 2]. It is important to note that these early publications provided a direct demonstration of the ability to employ heavy plastic straining in the production of bulk materials having fairly homogenous and equiaxed microstructures with grain sizes in the submicrometer or nanometer ranges and with a high fraction of high-angle grain boundaries. By now, the formation of UFG structure by Severe plastic deformation (SPD) processing is shown in many metals and alloys. Furthermore, recently a number of other nanostructural features (twins, particles, and so on) have been revealed in SPD-processed materials. The type and the morphology of such nanostructured elements and their density determine the mechanical, chemical, and physical properties of bulk nanomaterials. Over the last few years, the studies of bulk nanostructured materials tend to be more and more oriented to the development of their advanced and superior properties, and in this case, the conception of nanostructural design plays a far more important role. For example, the critical parameter for bulk nanostructured metals and alloys produced by SPD together with the grain refinement to the nanosized range is the grain boundary structure because the boundaries can be formed as low- and high-angle, special and random, and equilibrium and non-equilibrium boundaries depending on the SPD processing regimes [3, 4]. Furthermore, boundaries having different structures exhibit different transport mechanisms (deformation, diffusion, etc.) including grain boundary sliding, which in turn leads to differences in the properties. In such a manner, this opens a new way for advancing the properties of UFG materials by appropriately tuning their grain boundary structures.

The concept of nanostructural design of materials is schematically illustrated in Fig. 2.1—the scheme modifies and further develops a well-known concept of contemporary creation of novel materials through the integration of theory and modeling, structure characterization, processing and synthesis, as well as the properties of studies. In addition, nanostructuring of bulk materials deals with a far larger number of structural parameters related to the grain size and shape, lattice defects in the grain interior, as well as with the grain boundary structure, and also

I. Sabirov et al., *Bulk Nanostructured Materials with Multifunctional Properties*,
SpringerBriefs in Materials, DOI 10.1007/978-3-319-19599-5_2

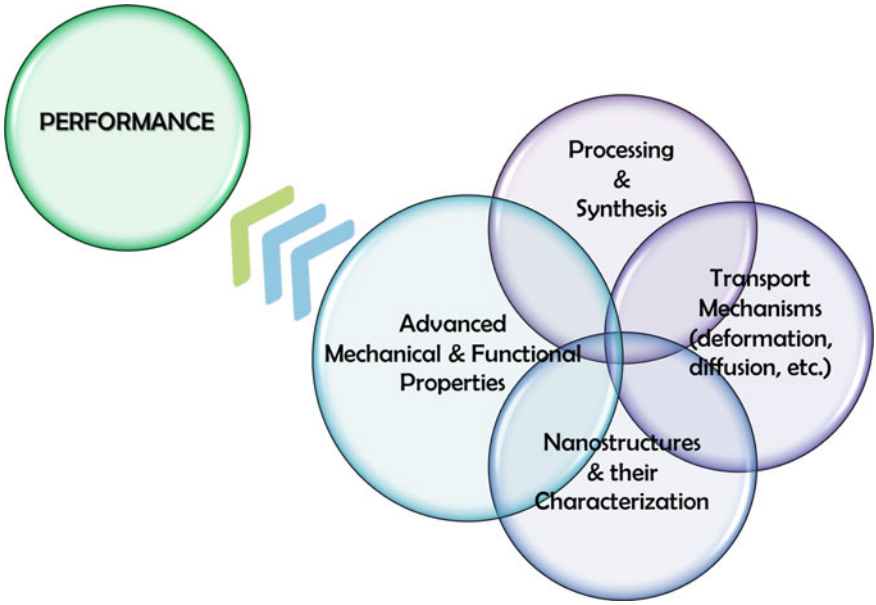

Fig. 2.1 Principles of nanostructural design of bulk nanostructured materials. The figure is reproduced from [5] with permission from the publisher

the presence of segregations and second-phase nanoparticles. This provides an opportunity to vary the transport mechanisms and therefore can drastically increase the properties. For example, nanostructuring of bulk materials by SPD processing not only permits a considerable enhancement of many mechanical and physical properties but also contributes to the appearance of multifunctional materials [6–10]. In this respect, one can anticipate that already in the near future, nanostructuring of materials by various processing and synthesis techniques may provide many new examples in the development of materials with superior properties for advanced structural and functional applications.

This book is devoted specifically to bulk nanostructured metallic materials produced by SPD. In recent years, a breakthrough has developed in studies of nanostructured metals and alloys as advanced structural and functional materials, associated both with the development of new routes for the fabrication of bulk nanostuctured materials using SPD and with investigations of the fundamental mechanisms that lead to the new properties of these materials.

The main nanostructural elements produced in the materials subjected to SPD processing, we consider in more detail below. In general, it is possible to identify four types of nanostructured elements in metals and alloys subjected to SPD that can be observed through the application of modern techniques of structural analysis such as high-resolution transmission electron microscopy (HRTEM) and 3D-atom probe [4, 11–14].

2.1 Grain Refinement via Severe Plastic Deformation

As it was mentioned above, SPD techniques have been used mostly because of their ability to produce UFG metallic materials through microstructure refinement in initially coarse-grained materials. The final grain size produced depends strongly on both processing regimes and the type of material. For pure metals, the mean grain size is typically about 100–200 nm after processing by HPT and about 200–300 nm after processing by ECAP or other techniques. For alloys and intermetallics, the grain size is usually smaller, and in some cases, it is in the range of 50–100 nm.

For the formation of UFG structures with primarily high-angle grain boundaries through SPD processing, five basic rules for grain refinement have been defined [15], four of which are related to the requirements for SPD processing regimes and routes, while the fifth is related to the intrinsic nature of the material under study. These rules are briefly considered below. A detailed description of SPD processing regimes and routes may be found in recent overviews on the subject [12, 16–18].

SPD processing at low temperatures (as a rule, less than 0.4 T_m) is referred to as a rather important requirement for its realization. Only under these conditions is it possible to achieve dislocation densities of 10^{14} m^{-2} or higher, up to the limiting values of 10^{16}–10^{17} m^{-2} [16, 19], which is necessary for the formation of the UFG structure. Higher processing temperatures result in a lower accumulated dislocation density and an increase in grain size above 1 μm.

The degree of strain during processing (true strain) should exceed 6–8. Although a considerable refinement of the microstructure and the attainment of dislocation densities exceeding 10^{14} m^{-2} occur at a strain of 1–2 [16], the formation of UFG structures with a majority of high-angle grain boundaries requires further straining.

High hydrostatic pressures, usually >1 GPa, are important for efficient SPD processing. High pressure contributes to the enhancement of deformability of the processed material and, therefore, provides solidity of the billets even under high strain [12, 20]. Furthermore, the pressure affects the diffusion and thus suppresses the annihilation of deformation-induced lattice defects [21].

The formation of equiaxed ultrafine grains depends on the vorticity of the metal flow. At the macrolevel, the vorticity is related to the non-monotonous character of deformation. For example, the ECAP with route B_C, in which the billet is rotated by 90° between each pass, is considerably more effective for grain refinement by comparison with route C, in which the billet position does not change [12]. At the microlevel, the vorticity is associated with grain rotations and displacements [22].

Grain refinement is also related to the atomic structure of the material processed. The ordering of alloys or low stacking fault energy (SFE), all other conditions being equal, contributes to the enhancement of an accumulated dislocation density and considerably reduces the grain size produced [16]. For example, for Pd–20 % Ag alloy with SFE = 125 mJ m^{-2}, in comparison with pure Pd with SFE = 190 mJ m^{-2}, during HPT (5 rotations under P = 6 GPa), the grain size produced equals 150 nm for Pd–20 % Ag and 240 nm for Pd, respectively [23].

These five rules are required and typically sufficient conditions for effective grain refinement by SPD processing.

2.2 Grain Boundaries in Nanostructured Materials

With grain sizes in a submicron (100–1000 nm) or nanocrystalline (<100 nm) range, UFG materials contain in their microstructure a very high density of grain boundaries, which can play a significant role in the development and exhibition of novel properties. For this reason, UFG materials can be typically considered as interface-controlled materials [24].

Already in first works on nanocrystalline materials pioneered by Gleiter and colleagues, it was suggested that grain boundaries can possess a number of peculiar features in terms of their atomic structure in contrast to grain boundaries in conventional polycrystalline materials [24, 25]. This is of particular importance for UFG materials produced by SPD methods.

Depending on the regimes of SPD processing, different types of grain boundaries can be formed in the UFG materials (high- and low-angle, special and random, and equilibrium and so-called non-equilibrium grain boundaries containing extrinsic dislocations) [16, 26], which paves the way to grain boundary engineering of UFG materials, i.e., to the control of their properties by means of varying the grain boundary structure.

The notions on non-equilibrium grain boundaries were first introduced in the scientific literature in the 1980s [27, 28] reasoning from investigations of interactions of lattice dislocations with grain boundaries. According to [28], the formation of a non-equilibrium grain boundary state is characterized by three main features, namely excess grain boundary energy (at the specified crystallographic parameters of the boundary), the presence of long-range elastic stresses (Fig. 2.2), and enhanced free volume. Discontinuous distortions of crystallographically ordered structures, which may come about by accommodation problems of differently oriented crystallites of finite sizes or by high densities of lattice dislocations and their interaction with grain boundaries, can be considered as sources of elastic stress fields that modify the atomic structure of high-angle grain boundaries so that their excess free energy becomes enhanced. These ‘unusual’ grain boundaries have been termed ‘non-equilibrium’ grain boundaries although in a strict sense, each grain boundary is a non-equilibrium defect if segregation effects (see Sect. 2.4) are not to be considered. Since, however, the term has been accepted and utilized by the entire community who works on severe plastic deformation, we also use it here, describing as ‘grain boundaries’ with strain distorted structures.

A model for these non-equilibrium grain boundaries has been developed by Nazarov, Romanov, and Valiev in a series of papers [29, 30] processing on their formation and behavior. Lattice dislocations that are created during the plastic straining move toward high-angle grain boundaries on their respective glide planes during continued straining and then, when reaching a high-angle grain boundary, transform into so-called extrinsic grain boundary dislocations, i.e., dislocations that do not contribute toward the misorientation of the two adjacent grains. As a net effect, high-angle grain boundaries with high densities of such extrinsic grain

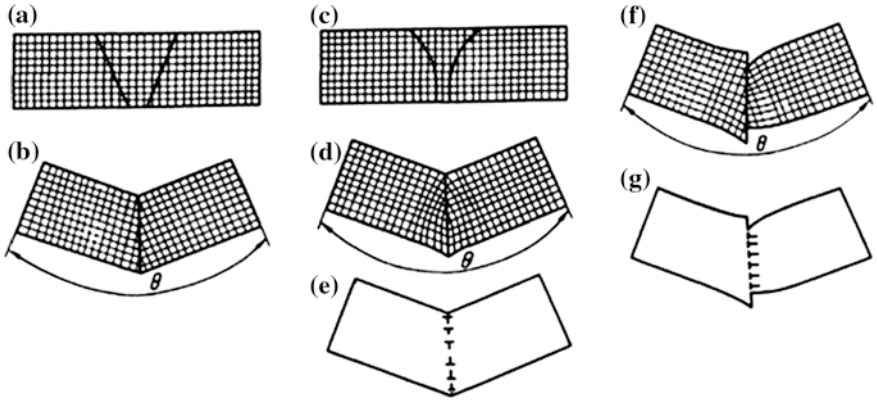

Fig. 2.2 Phenomenological engineering of grain boundaries via thought cuts: **a**→**b** equilibrium grain boundary (bunches of deformation are connected without mesoscopic strain); **c**→**d** and **a**→**f** non-equilibrium grain boundaries (deformation is required for crystal joint–bending and tension–compression, respectively); **e** and **g** schemes of grain boundary dislocation (GBD) complexes initiating the same character of mesoscopic elastic distortions as in (**d**) and (**f**). The figure is reproduced from [28] with permission from the publisher

boundary dislocations would also contain increased energy and free volume and considerable microstrain associated with the grain boundary region [29].

In earlier studies of grain boundaries in UFG materials processed by SPD techniques, there have been already used various, often mutually complementary, structural methods: transmission electron microscopy (TEM), X-ray diffraction, Mössbauer spectroscopy, dilatometry, differential calorimetry, and others (see, e.g., [16]). They clearly evidenced that mostly high-angle grain boundaries leading to grain refinement can be formed after optimization of SPD processing routes and these grain boundaries possess specific non-equilibrium structures. Later, structure-sensitive probes have been applied that are sensitive to modifications of the atomic structure, such as grain boundary diffusion measurements or HRTEM analyses, in order to identify and characterize transformations of the grain boundary structure due to the severe deformation processing.

For example, as illustrated in Fig. 2.3 [31], an excessively high density of dislocations, facets, and steps are observed at grain boundaries of the UFG alloy Al–3 % Mg after HPT that leads to a non-equilibrium state of boundaries with a crystal lattice distortion zone of ∼5–7 nm in width [32, 33] and which considerably influences the properties of the alloy. Non-equilibrium grain boundaries are typical for different materials after SPD processing, and their role in the mechanical behavior of UFG materials is observed in a number of reports [33, 34].

Horita et al. [31] and Valiev et al. [16] noticed also serrated contrast features in bright field TEM images and also in HRTEM analyses, respectively, that were interpreted as evidence for a high local density of dislocation structures associated with the apparent non-equilibrium grain boundary. However, due to the possible Moiré effect occurring in the projection of sample regions near interfaces and due to

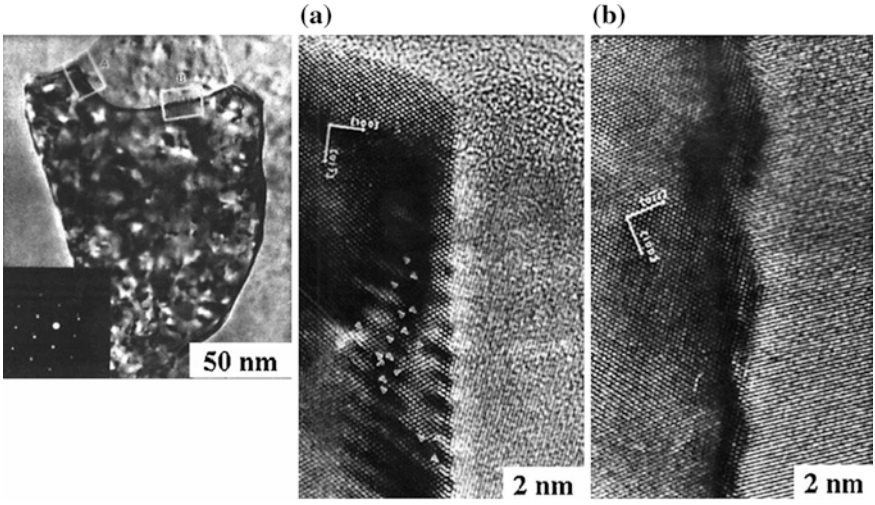

Fig. 2.3 TEM images of non-equilibrium grain boundaries in the UFG Al–3 % Mg alloy with a grain size of ~100 nm illustrating high-resolution photographs of regions *A* and *B*. The images are reproduced from [31] with permission from the publisher

the delocalization of information in HRTEM analyses by aberrations of the electromagnetic lenses, unambiguous interpretations of grain boundary structures require more sophisticated analyses, which today can be provided by the use of so-called Cs-corrected TEMs that are corrected for spherical aberration. Figure 2.4a shows the HRTEM image of a grain boundary with both adjacent grains oriented with their <110> zone axis parallel to the electron beam in a Pd90Ag10 alloy that had been severely deformed by repeated rolling and folding. The details of the synthesis process are similar to the procedure described earlier [35, 36]. The image was taken with a FEI-Titan TEM equipped with a field emission cathode and a Cs-corrector. The non-equilibrium character of this grain boundary in term of the interpretations given earlier by Valiev et al. is manifested in the non-uniform faceted form (Fig. 2.4a) of the two joining <110>-oriented grains. Grain boundaries with similar features are commonly observed for materials after SPD processing [37]. Yet, it should be noted that not all grain boundaries in severely deformed materials present morphologies as in Fig. 2.4a. In fact, only a minority of grain boundaries with an average spacing of a few grain diameters display non-uniform faceting, implying that also during SPD processing, the localization of deformation controls the evolution of the microstructure.

In order to analyze whether the non-uniformly faceted grain boundaries might correspond to non-equilibrium grain boundaries, the residual microstrain present at the grain boundary shown in Fig. 2.4a was analyzed by the method of geometric phase analysis (GPA) that allows calculating relative magnitudes of the in-plane components of the strain tensor and of the tensor of rigid body rotation with respect to a reference lattice, based on the intensity distribution in high-resolution electron

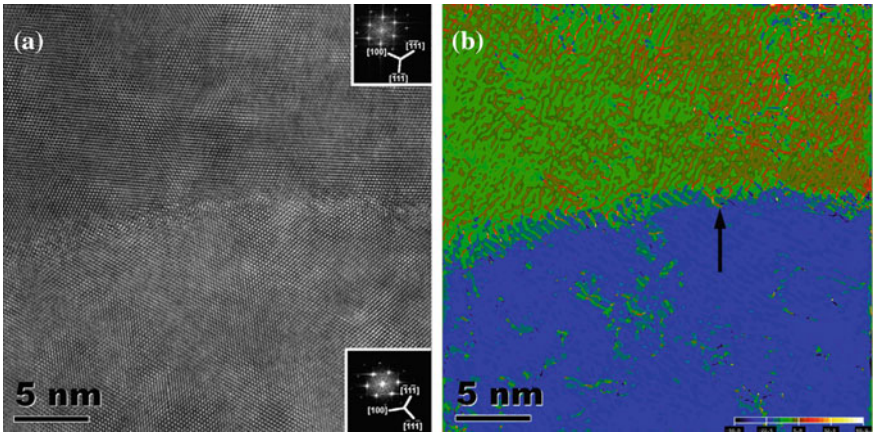

Fig. 2.4 **a** HRTEM micrograph showing two adjacent grains of Ag10Pd90 (after 110 cycles) both oriented along the <110> direction. The grains are rotated by an angle of 23.7° with respect to each other. The grain boundary appears here in a wavy faceted form. The Fourier transforms of the images of both grains are given as inserts. **b** Strain map showing the in-plane rigid body rotation xy [rotations on a scale from −50° (*dark blue*) to +60° (*yellow-white*) (anticlockwise positive) are displayed]. Hot spots (see *arrow* pointing on one example) in *bright yellow color* (where the phase of the electron wave changed discontinuously), which are discernible at high density along the GB if examined at higher magnification, refer to dislocation cores. The *greenish color* of the upper grain represents the zero rotation taken as a reference. The images are reproduced from [40] with permission from the publisher

micrographs [38, 39]. Details concerning the analysis and concerning the conditions under which the HRTEM micrograph was taken can be found in [40]. One result of this analysis is displayed in Fig. 2.4b as the rigid body rotation. In addition to the misorientation between the two neighboring grains, a clear and significant variation of the color representing the variation of the relative rotations of the lattice is observed in the near-boundary region. It should be noted that the bright spots ('hot spots') in Fig. 2.4b represent regions where a discontinuity in the transmitted phase of the electron wave occurs, i.e., these spots mark the positions of the core region of full or partial dislocations. Additionally, local structures within the distorted grain boundary region that show an abrupt change in the local orientation of the crystal lattice with respect to the orientation of the lattice of the parent grain could also contribute such bright features in the strain maps, since the linear density of the hot spots that is estimated to be about 10^9 m^{-1} is obviously much too high to be associated with the extrinsic GB dislocations only.

Thus, with respect to the grain boundary structure in SPD-processed materials with ultrafine grain size, recent studies enable to conclude that

- Non-equilibrium grain boundaries with strain distorted structure exist in UFG materials, and these specific grain boundaries possess an increased free-energy density, increased width, high density of dislocations (full or partial) associated with the near-boundary region, and correspondingly large residual microstrain.

- The structural width of non-equilibrium grain boundaries is about several nanometers, and it seems significantly larger than the width of relaxed high-angle grain boundaries in annealed coarse-grained materials.

2.3 Nanotwins in Metallic Materials After Severe Plastic Deformation

It is well known that contrary to coarse-grained metals, which become more difficult to twin with decreasing grain size, nanocrystalline face-centered-cubic (fcc) metals become easier to twin with decreasing grain size, reaching a maximum twinning probability, and then become more difficult to twin when the grain size decreases further, i.e., exhibiting an inverse grain-size effect on twinning. Molecular dynamics simulations and experimental observations have revealed that the mechanisms of deformation twinning in nanocrystalline metals are different from those in their coarse-grained counterparts. Consequently, there are several types of deformation twins that are observed in nanocrystalline materials, but not in coarse-grained metals [41]. It has also been reported that deformation twinning can be utilized to enhance the strength and ductility of nanocrystalline materials.

In particular, nanotwins are typical of the materials after ECAP at lower temperatures and/or those subjected to additional cold rolling (CR), extrusion, or drawing. Figure 2.5 shows a TEM image of atom resolution of UFG Cu after ECAP and CR at liquid nitrogen temperature with clearly observed twins of 10–20 nm in size [42]. Such nanostructured defects also have a considerable effect on material strength by, for example, increasing the yield stress (YS) in UFG Cu from ~380 to ~510 MPa [42, 43].

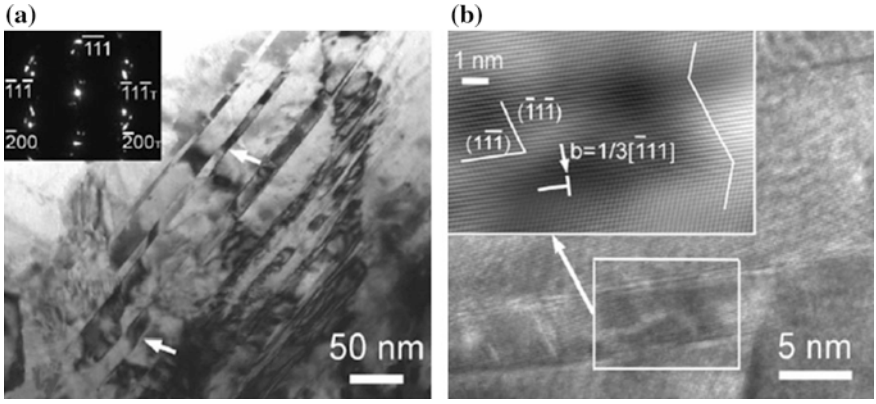

Fig. 2.5 TEM images at **a** low and **b** high magnifications of a typical grain with a high density of deformation twins in UFG Cu processed by ECAP with subsequent cold rolling. The images are reproduced from [42] with permission from the publisher

2.4 Segregations in Nanostructured Alloys Processed by Severe Plastic Deformation

Indirect evidence of grain boundary segregation in UFG materials processed by SPD has been reported in a few cases where the thermal stability has been investigated as a function of the impurity level in Ni [44] or as a function of the concentration of Sb in Cu [45]. However, only recently, reports providing direct evidence of grain boundary segregation in UFG materials processed by SPD have appeared. Most of them rely on atomic scale characterization thanks to atom probe tomography (APT). This technique provides only very limited crystallographic information, and the grain boundary misorientation is usually unknown. Moreover, only small grain boundary areas can be analyzed making any statistics almost impossible. Anyway, it was demonstrated that grain boundary segregation in SPD-processed materials is not a marginal feature but could be observed in various kinds of alloys.

Grain boundary segregations were reported in an AA6061 processed by HPT [46] or ECAP [47] where Mg, Cu, and Si segregations along planar defects attributed to grain boundaries were observed. The solute element-enriched layer is about 2 nm, and the local enrichment does not exceed 2 at.%. Grain boundary segregations were also reported for an Al–Mg–Cu–Zn alloy processed by ECAP (Fig. 2.6) [14], an AA7075 processed by HPT [48], and an Al–6.8 % Mg processed by HPT [49]. In the HPT processed AA7075 (20 turns), a mean grain size of about 100 nm is achieved, with a large fraction of high-angle grain boundaries. Using APT, very strong Mg local enrichments up to 25 at.% in a much thicker layer (6–8 nm) were observed (Fig. 2.7). This thickness is much larger than the grain boundary width measured on HRTEM images thanks to GPA (about 2 nm), where this parameter was defined as a zone where the averaged rotational component of

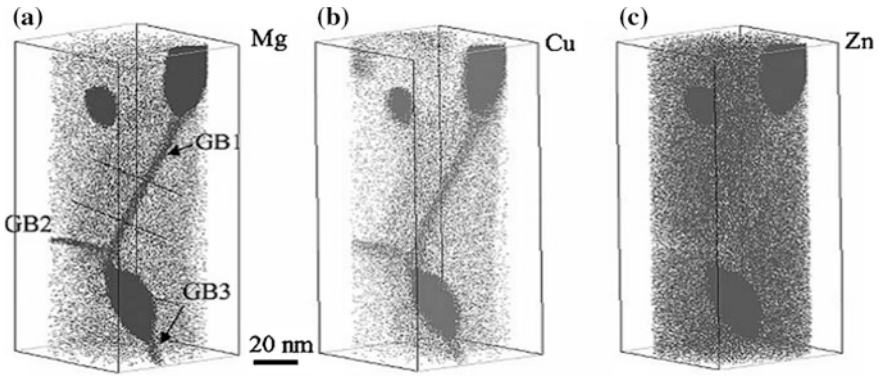

Fig. 2.6 Elemental maps of polycrystalline region of an Al–Zn–Mg–Cu alloy after 8 passes of ECAP. **a** Mg, **b** Cu, and **c** Zn maps. The figure is reproduced from [14] with permission from the publisher

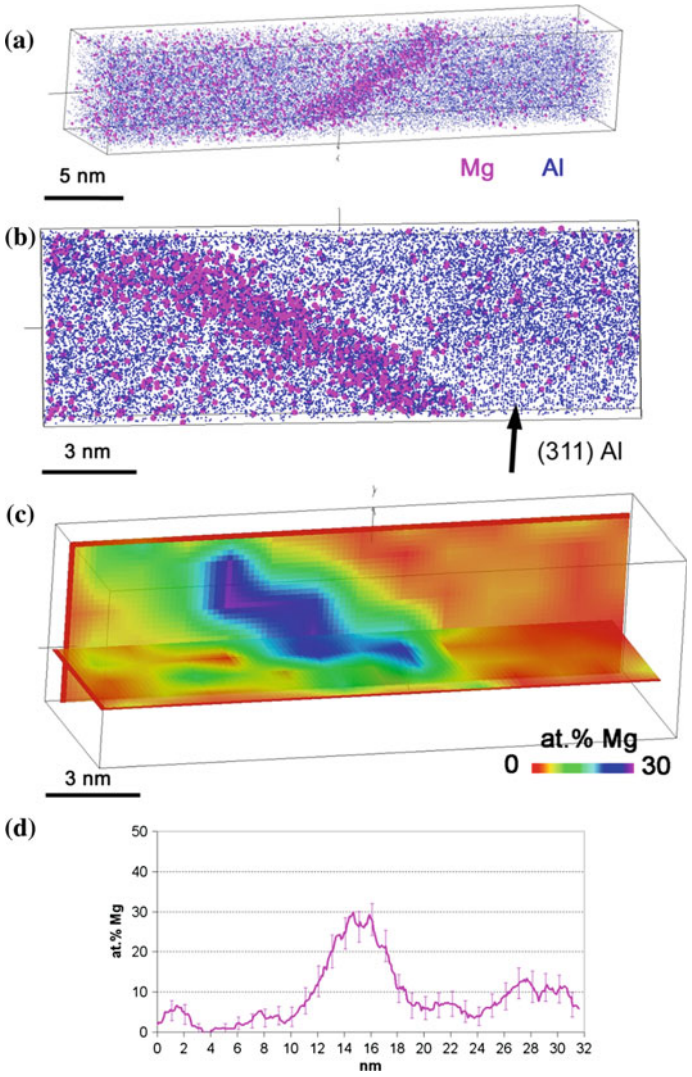

Fig. 2.7 3D reconstruction of an analyzed volume in the UFG 1570 alloy: **a** full data set showing a planar segregation of Mg (Al atoms are displayed as dots and Mg atoms as bubbles); **b** selected part orientated to display (311)Al atomic planes on the right of the planar segregation; **c** 2D chemical map showing the Mg concentration fluctuations within the volume; **d** concentration profile computed across the segregation (sampling volume thickness 1 nm). The figure is reproduced from [49] with permission from the publisher

the strain field is changed from the value in one grain to that in its neighbor. It seems a non-equilibrium grain boundary may incorporate a larger amount of segregating atoms with respect to relaxed interfaces (as a result of the increased free volume), but the thickness of the segregated layer might not only be determined by

the distorted layer near the non-equilibrium GB (as it is defined by GPA). APT data also revealed that grain boundaries are not homogeneously covered and that the Mg concentration in solid solution may strongly vary from one grain to another [49]. Such features might indicate that the local configuration of the GB and especially dislocations lying in the vicinity of the boundaries may affect the distribution of solute elements. It is also interesting to note that this material exhibits a very high YS after HPT processing, much higher than a prediction based on the Hall–Petch law. Thus, it seems that GB segregations could significantly affect the deformation mechanisms (dislocation nucleation and glide) in nanostructured metallic materials processed by SPD.

2.5 Precipitation of Second Phases in Alloys During and/or After Severe Plastic Deformation

The formation of particles has been observed in many alloys subjected to SPD after solution quenching [11, 12]. Figure 2.8 illustrates an example of such nanoparticles ~10–20 nm in size precipitated in the UFG AA6061 after ECAP-PC processing [50]. The presence of nanoparticles is related to dynamic aging and provides additional precipitation hardening of the alloys [12, 50]. However, the size and morphology of precipitates are usually closely related to the SPD processing parameters. Recently, this approach has been used for the development of a new strategy for nanostructural design in the Al alloys for the new generation conductors [52]. This strategy is based on intelligent manipulation with the strengthening mechanisms and mechanisms of electrical resistivity by grain refinement down to submicrometer scale, using SPD processing at room temperature, followed by

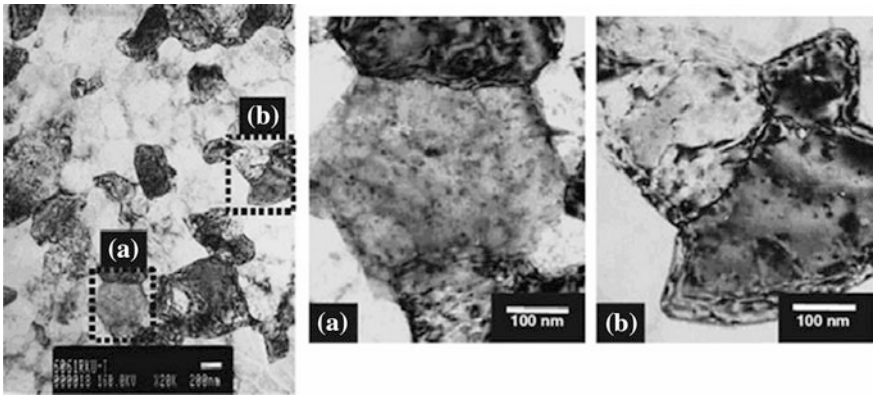

Fig. 2.8 UFG structure of an AA6061 after ECAP with parallel channels (four passes): The formation of nanosized precipitations is clearly visible inside the grain after processing in areas *A* and *B*

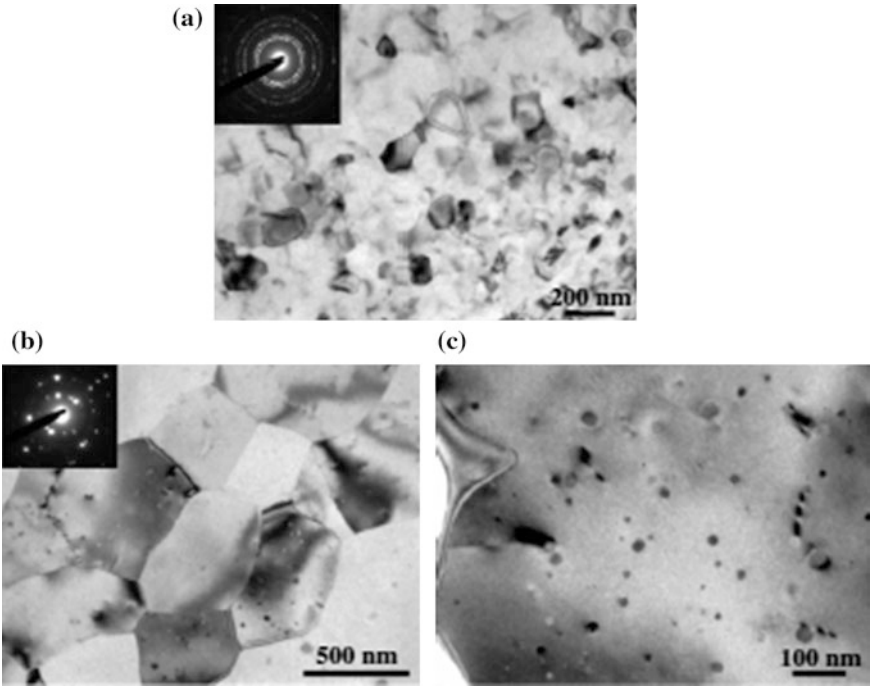

Fig. 2.9 TEM images of the AA6201 subjected to HPT processing at: **a** RT; **b**, **c** 180 °C. **a**, **b** General view of UFG structures, and **c** morphology of precipitates

decomposition of supersaturated solid solution and formation of nanosized second-phase precipitates via dynamic aging during SPD processing at elevated temperatures. These ultrafine-grained (UFG) microstructures with second-phase nanoprecipitates can show superior mechanical strength owing to grain boundary strengthening and precipitation hardening. At the same time, the very low content of solute atoms and the absence of GP zones in the Al matrix result in significantly enhanced electrical conductivity. For experiment, an AA6201 was chosen, which has been widely used as a material for electroconductors [52]. Disks with diameter 20 mm and thickness 1.5 mm were solution treated at 530 °C for 2 h and quenched in water. Then, the disks were subjected to SPD processing by high-pressure torsion (HPT) using unconstrained anvils [17]. Several processing parameters were selected: room temperature (RT) and further straining at 130, 180, and 230 °C. The disks were subjected to one HPT turn at room temperature followed by 20 HPT turns at elevated temperatures.

Careful TEM studies have shown that the alloy processed at RT exhibits a very homogeneous UFG microstructure with a mean grain size of $\sim$130 nm (Fig. 2.9a). The grain interior is characterized by a low density of lattice dislocations. Meanwhile, spreading of spots on selected area electron diffraction patterns and extinction lines inside grains point to the high residual stresses present as a result of

the non-equilibrium character of grain boundaries containing extrinsic dislocations [4, 31].

Further HPT straining at elevated temperatures significantly affects the UFG microstructure (Fig. 2.9b). The results of microstructural characterization of the HPT processed AA6201 alloy are presented in Table 2.1. The mean grain size in the alloy increases to 280, 440, and 960 nm after HPT processing at 130, 180, and 230 °C, respectively (Table 2.1). A very important feature of these microstructures is the presence of spherical second-phase nanoprecipitates (Fig. 2.9c). The average size of the second-phase precipitates increases with increasing HPT processing temperature from 10 nm (at 130 °C) to 50 nm (230 °C) (Table 2.1). These nanoprecipitates have been identified as β-Mg_2Si, and they are typically formed as a result of dynamic aging, which occurs during SPD processing of the Al–Mg–Si alloys at elevated temperatures [51, 53, 54]. It should be noted that these nanoprecipitates have a different morphology compared with the nanoprecipitates formed in the material during static aging, which have a needle shape. This was attributed to the strong dislocation activity during SPD processing and the resulting shear of precipitates [52, 53]. The X-ray measurements clearly show that HPT processing leads to a significant decrease in the lattice parameter of the Al matrix (Table 2.1) illustrating a strong decomposition of the supersaturated solid solution. This is in a good accordance with the results of the recent investigations using the 3D APT technique [4]. The lattice parameter in the alloys processed at 230 °C becomes nearly equal to that of the pure Al (4.0494 Å), which indicates near-complete purification of the matrix from the solute atoms as a result of dynamic aging (Table 2.1). The appearance of typical banded diffraction contrast at grain boundaries indicates significant recovery of non-equilibrium grain boundaries during HPT at elevated temperatures (Fig. 2.9b) [32].

From this Chapter, it is seen that manipulation with the SPD processing parameters provides a powerful tool for nanostructural design in the metallic materials. Basically, all microstructural parameters (grain size, grain boundary state, dislocations density, nanosegregations of solute atoms, etc.) can be controlled in the SPD-processed materials in order to tailor their mechanical and functional properties. The effect of microstructure on the properties of the nanostructured metallic materials via SPD is considered in the next chapter.

Table 2.1 Microstructure and mechanical properties of the AA6201 alloy in the studied conditions

Processing	Microstructure	α [Å]
Solid solution treated	CG; d = 65 μm	4.0526
T81	CG; d = 65 μm	4.0512
HPT at room temperature	UFG; d = 130 nm	4.0521
HPT at room temperature + HPT at 130 °C	UFG; d = 130 nm, d_p = 10 nm	4.0509
HPT at room temperature + HPT at 180 °C	UFG; d = 130 nm, d_p = 30 nm	4.0505
HPT at room temperature + HPT at 230°C	UFG; d = 130 nm, d_p = 50 nm	4.0500

d grain size; d_p size of second-phase precipitates; α lattice parameter

References

1. Valiev, R.Z., Krasilnikov, N.A., Tsenev, N.K.: Plastic deformation of alloys with submicron-grained structure. Mater. Sci. Eng. A **137**, 35 (1991)
2. Valiev, R.Z., Korznikov, A.V., Mulyukov, R.R.: Structure and properties of ultrafine-grained materials produced by severe plastic deformation. Mater. Sci. Eng. A **186**, 141 (1993)
3. Valiev, R.Z.: Nanostructuring of metals by severe plastic deformation for advanced properties. Nat. Mater. **3**, 511 (2004)
4. Sauvage, X., Wilde, G., Divinski, S.V., Horita, Z., Valiev, R.Z.: Grain boundaries in ultrafine grained materials processed by severe plastic deformation and relared phenomena. Mater. Sci. Eng. A **1**, 540 (2012)
5. Suresh, S. (ed.): The millennium special issue. A selection of major topics in materials science and engineering: current status and future directions. Acta Mater. **48**, 1–384 (2000)
6. Ivanisenko, Y., Darbandi, A., Dasgupta, S., Kruk, R., Hahn, H.: Bulk nanostructured materials: non-mechanical synthesis. Adv. Eng. Mater. **12**, 666 (2010)
7. Horita, Z.: In: Horita, Z. (ed.) Proceedings of International Symposium on Giant Straining Process for Advanced Materials, Fukuoka (2011)
8. Sabirov, I., Murashkin, M.Y., Valiev, R.Z.: Nanostructured aluminium alloys produced by severe plastic deformation: new horizons in development. Mater. Sci. Eng. A **560**, 1 (2013)
9. Valiev, R.Z., Langdon, T.G.: The art and science of tailoring materials by nanostructuring for advanced properties using SPD techniques. Adv. Eng. Mater. **12**, 677 (2010)
10. Estrin, Y., Vinogradov, A.V.: Extreme grain refinement by severe plastic deformation: a wealth of challenging science. Acta Mater. **61**, 782 (2013)
11. Valiev, R.Z., Alexandrov, I.V.: Bulk Nanostructured Metallic Materials: production, structure and properties, p. 398. Moscow, Akademkniga Pub (2007)
12. Valiev, R.Z., Langdon, T.G.: Principles of equal-channel angular pressing as a processing tool for grain refinement. Prog. Mater Sci. **51**, 881 (2006)
13. Nurislamova, G., Sauvage, X., Murashkin, M., Islamgaliev, R., Valiev, R.Z.: Nanostructure and related mechanical properties of an Al-Mg-Si alloy processed by severe plastic deformation. Philos. Mag. Lett. **88**, 459 (2008)
14. Sha, G., Wang, Y.B., Liao, X.Z., Duan, Z.C., Ringer, S.P., Langdon, T.G.: Influence of equal-channel angular pressing on precipitation in an Al–Zn–Mg–Cu alloy. Acta Mater. **57**, 3123 (2009)
15. Valiev, R.Z.: Nanostructuring of metallic materials by SPD processing for advanced properties. Int. J. Mater. Res. **100**, 757 (2009)
16. Valiev, R.Z., Islamgaliev, R.K., Alexandrov, I.V.: Bulk nanostructured materials from severe plastic deformation. Prog. Mater Sci. **45**, 103 (2000)
17. Zhilyaev, A.P., Langdon, T.G.: Using high-pressure torsion for metal processing: fundamentals and applications. Prog. Mater Sci. **53**, 893 (2008)
18. Valiev, R.Z., Zhilyaev, A.P., Langdon, T.G.: Bulk Nanostructured Materials: Fundamentals and Applications. Wiley, New York (2014)
19. Ungar, T., Balogh, L., Zhu, Y.T., Horita, Z., Xu, C., Langdon, T.G.: Using X-ray microdiffraction to determine grain sizes at selected positions in disks processed by high pressure torsion. Mater. Sci. Eng. A **444**, 153 (2007)
20. Valiev, R.Z., Estrin, Y., Horita, Z., Langdon, T.G., Zehetbauer, M.J., Zhu, Y.T.: Producing bulk ultrafine-grained materials by severe plastic deformation. JOM **58**(4), 33 (2006)
21. Zehetbauer, M.J.: Nanomaterials by severe plastic deformation (SPD). Adv. Eng. Mater. **5**, 251916-1–251916-3 (2003)
22. Gutkin, M.Y., Ovidko, I.A.: Grain boundary migration as rotational deformation mode in nanocrystalline materials. Appl. Phys. Lett. **87**, 251916-1 (2005)
23. Kurmanaeva, L., Ivanisenko, Yu., Markmann, J., Kubel, C., Chuvilin, A., Doyle, S., Valiev, R.Z., Fecht, H.-J.: Grain refinement and mechanical properties in ultrafine-grained Pd and Pd–Ag alloys produced by HPT. Mater. Sci. Eng. A **527**, 1776 (2010)

24. Gleiter, H.: Nanocrystalline materials. Prog. Mater. Sci. **33**, 223 (1989)
25. Gleiter, H.: Nanostructured materials: basic concepts and microstructure. Acta Mater. **48**, 1 (2000)
26. Valiev, R.Z.: On grain boundary engineering of UFG metals and alloys for enhancing their properties. Mater. Sci. Forum **22**, 584–586 (2008)
27. Grabski, M.W.: Mechanical properties of internal interfaces. J. Phys. **46**(C4/4), 567 (1985)
28. Valiev, R.Z., Gertsman, VYu., Kaibyshev, O.A.: Grain boundary structure and properties under external influences. Phys. Stat. Sol. A **97**(11), 11 (1986)
29. Nazarov, A.A., Romanov, A.E., Valiev, R.Z.: On the structure, stress fields and energy of non-equilibrium grain boundaries. Acta Metall. Mater. **41**, 1033 (1993)
30. Nazarov, A.A., Romanov, A.E., Valiev, R.Z.: Incorporation model for the spreading of extrinsic grain boundary dislocations. Scripta Metall. Mater. **24**, 1929 (1990)
31. Horita, Z., Smith, D.J., Furukawa, M., Nemoto, M., Valiev, R.Z., Langdon, T.G.: An investigation of grain boundaries in submicrometer-grained Al-Mg solid solution alloys using high-resolution electron microscopy. J. Mater. Res. **11**, 1880 (1996)
32. Valiev, R.Z., Islamgaliev, R.K., Alexandrov, I.V.: Bulk nanostructured materials from severe plastic deformation. Prog. Mater Sci. **45**, 103 (2000)
33. Valiev, R.Z., Nazarov, A.A.: In: Zehetbauer, M.J., Zhu, Y.T. (eds.) Bulk Nanostructured Materials, p. 21. Wiley-VCH Verlag GmbH&Co. KGaA, Weinheim (2009)
34. Valiev, R.Z., Kozlov, E.V., Ivanov, YuF, Lian, J., Nazarov, A.A., Baudelet, B.: Deformation behaviour of ultra-fine-grained copper. Acta Metall. Mater. **42**, 2467 (1994)
35. Dinda, G.P., Rösner, H., Wilde, G.: Synthesis of bulk nanostructured Ni, Ti and Zr by repeated cold-rolling. Scripta Mater. **52**, 577 (2005)
36. Wilde, G., Rösner, H., Dinda, G.P.: Synthesis of bulk nanocrystalline materials by repeated cold-rolling. Adv. Eng. Mater. **7**, 11 (2005)
37. Divinski, S.V., Reglitz, G., Rösner, H., Wilde, G., Estrin, Y.: Self-diffusion in Ni prepared by severe plastic deformation: effect of non-equilibrium grain boundary state. Acta Mater. **59**, 1974 (2011)
38. Hÿtch, M.J., Snoeck, E., Kilaas, R.: Quantitative measurement of displacement and strain fields from HREM micrographs. Ultramicroscopy **74**, 131 (1998)
39. Rösner, H., Boucharat, N., Padmanabhan, K.A., Markmann, J., Wilde, G.: Strain mapping in a deformation-twinned nanocrystalline Pd grain. Acta Mater. **58**, 2610 (2010)
40. Wilde, G., Ribbe, J., Reglitz, G., Wegner, M., Rösner, H., Estrin, Y., Zehetbauer, M., Setman, D., Divinski, S.: Plasticity and grain boundary diffusion at small grain sizes. Adv. Eng. Mater. **12**, 758 (2010)
41. Zhu, Y.T., Liao, X.Z., Wu, X.L.: Deformation twinning in nanocrystalline materials. Prog. Mater Sci. **57**, 1–62 (2012)
42. Zhao, Y., Bingert, J.F., Liao, X., Cui, B., Han, K., Sergueeva, A.V., Mukherjee, A.K., Valiev, R.Z., Langdon, T.G., Zhu, Y.T.: Simultaneously increasing the ductility and strength of ultra-fine-grained pure copper. Adv. Mater. **18**, 2949 (2006)
43. Chukin, M.V., Koptseva, H.V., Valiev, R.Z., Yakovleva, I.L., Zrnik, G., Covarik, T.: The diffraction submicroscopic analysis of the submicrocrystal and nanocrystal structure of constructional carbon steels after equal channel angle pressing and further deformation. Vestnik MGTU **1**, 31 (2008)
44. Zhang, H.W., Huang, X., Pippan, R., Hansen, N.: Thermal behavior of Ni (99.967 % and 99.5 % purity) deformed to an ultra-high strain by high pressure torsion. Acta Mater. **58**, 1698 (2010)
45. Rajgarhia, R.K., Saxena, A., Spearot, D.E., Hartwig, K.T., More, K.L., Kenik, E.A., Meyer, H.: Microstructural stability of copper with antimony dopants at grain boundaries: experiments and molecular dynamics simulations. J. Mater. Sci. **45**, 6707 (2010)
46. Nurislamova, G., Sauvage, X., Murashkin, M., Islamgaliev, R., Valiev, R.: Nanostructure and related mechanical properties of an Al-Mg-Si alloy processed by severe plastic deformation. Phil. Mag. Lett. **88**, 459 (2008)

47. Sauvage, X., Murashkin, MYu., Valiev, R.Z.: Atomic scale investigation of dynamic precipitation and grain boundary segregation in a 6061 aluminium alloy nanostructured by ECAP. Kovove Mater. **49**, 11 (2011)
48. Liddicoat, P.V., Liao, X.-Z., Zhao, Y., Zhu, Y.T., Murashkin, M.Y., Lavernia, E.J., Valiev, R. Z., Ringer, S.P.: Nanostructural hierarchy increases the strength of aluminium alloys. Nature Comm. **1**, 63 (2010)
49. Valiev, R.Z., Enikeev, N.A., Murashkin, MYu., Kazykhanov, V.U., Sauvage, X.: On the origin of extremely high strength of ultrafine-grained Al alloys produced by severe plastic deformation. Scripta Mater. **63**, 949 (2010)
50. Valiev, R.Z., Murashkin, MYu., Bobruk, E.V., Raab, G.I.: Grain refinement and mechanical behavior of the Al alloy subjected to the new SPD technique. Mater. Trans. **50**, 87 (2009)
51. Murashkin, MYu., Sabirov, I., Kazykhanov, V.U., Bobruk, E.V., Dubravina, A.A., Valiev, R. Z.: Enhanced mechanical properties and electrical conductivity in ultrafine-grained Al alloy processed via ECAP-PC. J. Mater. Sci. **48**, 4501 (2013)
52. Valiev, R.Z., Murashkin, MYu., Sabirov, I.: A nanostructural design to produce high strength Al alloys with enhanced electrical conductivity. Scripta Mater. **76**, 13–16 (2014)
53. Sauvage, X., Murashkin, MYu., Valiev, R.Z.: Atomic scale investigation of dynamic precipitation and grain boundary segregation in a 6061 aluminium alloy nanostructured by ECAP. Kovove Mater. **49**(1), 11 (2011)
54. Kim, W.J., Wang, J.Y., Choi, S.O., Choi, H.J., Sohn, H.T.: Synthesis of ultra high strength Al–Mg–Si alloy sheets by differential speed rolling. Mater. Sci. Eng., A **520**, 23 (2009)